On Smooth Orthogonal and Octilinear Drawings: Relations, Complexity and Kandinsky Drawings[☆]

Michael A. Bekos, Henry Förster*, Michael Kaufmann

Wilhelm-Schickhard-Institut für Informatik, Universität Tübingen
Sand 13, 72076 Tübingen, Germany

Abstract

We study two variants of the well-known orthogonal graph drawing model: (i) the smooth orthogonal, and (ii) the octilinear. Both models form an extension of the orthogonal one, by supporting one additional type of edge segments (circular arcs and diagonal segments, respectively).

For planar graphs of max-degree 4, we analyze relationships between the graph classes that can be drawn bendless in the two models and we also prove NP-hardness for a restricted version of the bendless drawing problem for both models. For planar graphs of higher degree, we present an algorithm that produces bi-monotone smooth orthogonal drawings with at most two segments per edge, which also guarantees a linear number of edges with exactly one segment.

Keywords: Graph drawing, smooth orthogonal, octilinear

1. Introduction

Orthogonal graph drawing is an intensively studied and well established model for drawing graphs [1, 2]. As a result, several efficient algorithms providing good aesthetics and good readability have been proposed over the years, see

[☆]A preliminary version of this article has appeared in the proceedings of the 25th International Symposium on Graph Drawing and Network Visualization.

*Corresponding author.

Email addresses: bekos@informatik.uni-tuebingen.de (Michael A. Bekos), foersth@informatik.uni-tuebingen.de (Henry Förster), mk@informatik.uni-tuebingen.de (Michael Kaufmann)

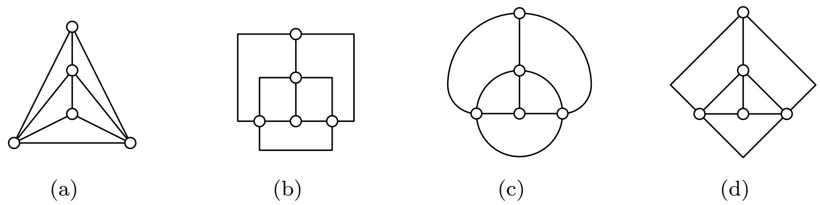

Figure 1: Different drawings of a planar graph of max-degree 4: (a) straight-line, (b) orthogonal 3-drawing, (c) smooth orthogonal 2-drawing, and (d) octilinear 2-drawing.

e.g., [3, 4, 5, 6]. In such drawings, each vertex corresponds to a point on the Euclidean plane and each edge is drawn as an alternating sequence of axis-aligned line segments; refer to Figure 1b for an example.

Several research directions build upon this successful model. In this work, we focus on two models that have recently received attention. The first one is the *smooth orthogonal* [7], in which every edge is a sequence of axis-aligned segments and circular arc segments with common axis-aligned tangents (i.e., quarter, half or three-quarter circular arc segments); refer to Figure 1c for an example. The second model is the *octilinear* [8], in which every edge is a sequence of axis-aligned and diagonal (at $\pm 45°$) segments; refer to Figure 1d for an example. In the orthogonal and in the smooth orthogonal models, each edge may enter a vertex using one out of four available (axis-aligned) directions, called *ports*. Thus both models support graphs of max-degree 4. In the octilinear model, each vertex has eight available ports that are equispaced around each vertex and therefore one can draw graphs of max-degree 8.

Observe that both models extend the orthogonal by allowing one more type of edge-segments (circular arcs and diagonal segments, respectively). The smooth orthogonal drawing model was introduced with the aim of combining the artistic appeal of *Lombardi drawings* [9, 10] with the clarity and rigidity of the orthogonal drawings. The octilinear drawing model, on the other hand, is primarily motivated by metro-map and map schematization applications (see, e.g., [11, 12, 13, 14]).

For readability purposes, usually in such drawings one seeks to minimize the *edge complexity* [1, 2], that is, the maximum number of segments used for representing any edge. Also, when the input is a planar graph, one seeks for a corresponding planar drawing. Note that drawings with edge complexity 1 are also called *bendless*. We refer to drawings with edge complexity k as k*-drawings*; thus, by definition, orthogonal and octilinear k-drawings have at most $k-1$ bends per edge.

Known results. There exists a plethora of results for each of the aforementioned models; here we overview existing results for drawings with low edge complexity. For a more detailed overview, we point the reader to [15].

- All planar graphs of max-degree 4, except for the octahedron, admit orthogonal 3-drawings; the octahedron is orthogonal 4-drawable [3, 5]. All planar graphs of max-degree 3 admit orthogonal 2-drawings [16]. Minimizing the number of bends over all embeddings of a planar graph of max-degree 4 is $\mathcal{NP}$-hard [17]. For a given planar embedding, however, finding a planar orthogonal drawing with minimum number of bends can be done in polynomial time by an approach, called *topology-shape-metrics* [6]. The core of this approach is based on min-cost flow computations and works in three phases. Initially, a planar embedding is computed unless specified by the input (*topology phase*). In the next phase, called *shape phase*, the angles and the bends of the drawing are computed, yielding an *orthogonal representation*. In the last phase, called *metrics phase*, the actual coordinates for the vertices and bends are computed. For more details, we point the reader to [18].

- All planar graphs of max-degree 4 (including the octahedron) admit smooth orthogonal 2-drawings. Note that not all planar graphs of max-degree 4 allow for bendless smooth orthogonal drawings [7], and that such drawings may require exponential area [19]. Bendless smooth orthogonal drawings are possible only for subclasses, e.g., for planar graphs of max-degree 3 [20] and for outerplanar graphs of max-degree 4 [19]. It is worth mentioning that the complexity of the recognition problem, whether a planar graph of max-degree 4 admits a bendless smooth orthogonal drawing, has not been settled (it is conjectured to be $\mathcal{NP}$-hard [19]).

- All planar graphs of max-degree 8 admit octilinear 3-drawings [21], while planar graphs of max-degree 4 and max-degree 5 allow for octilinear 2-drawings in cubic and super-polynomial area, respectively [8]. Bendless octilinear drawings are always possible for planar graphs of max-degree 3 [22, 23]. Note that deciding whether an embedded planar graph of max-degree 8 admits a bendless octilinear drawing is $\mathcal{NP}$-hard [12]. It is not, however, known whether this negative result applies for planar graphs of max-degree 4 or whether these graphs allow for a decision algorithm; in fact, there exist planar graphs of max-degree 4 that do not admit bendless octilinear drawings [24].

Our contribution. We study smooth orthogonal and octilinear drawings of planar graphs with small edge complexity. Our results are summarized as follows:

- Motivated by the fact that usually one can "easily" convert a smooth orthogonal drawing of a planar graph of max-degree 4 to a corresponding octilinear one (e.g., by replacing quarter circular arc segments with diagonal edge segments; see Figures 1c-1d for an example), and vice versa, we study in Section 3 inclusion-relationships between the graph-classes that admit such drawings. Our findings are also summarized in Figure 3.

- In Section 4, we show that it is $\mathcal{NP}$-hard to decide whether an embedded planar graph of max-degree 4 admits a bendless smooth orthogonal or a bendless octilinear drawing, in the case where the angles between any two edges incident to a common vertex and the shapes of all edges are specified as part of the input (e.g., as in the last step of the topology-shape-metrics approach [6]). Our proof is a step towards settling the complexities of both decision problems in their general form. Note that, our NP-hardness result shows that the last step of the topology-shape-metrics approach is hard, if considered in isolation in the smooth orthogonal model or in the octilinear model, while in the classic orthogonal model it can be solved efficiently using network flows. This observation suggests that the topology-shape-metrics approach is suitable for neither of the two models.

- Inspired from the *Kandinsky model* (see, e.g., [25, 26, 4]) for drawing planar graphs of arbitrary degree in an orthogonal style, we present in Section 5 two drawing algorithms that yield bi-monotone smooth orthogonal drawings of good quality. More precisely, the first yields drawings of quadratic area, which can also be transformed to octilinear with bends at 135°, while maintaining the area consumption asymptotically unchanged. The second algorithm yields drawings of cubic area but at the same time guarantees that at most $2n-5$ edges are drawn with two segments.

Before we proceed with the detailed description of our algorithms, we introduce in Section 2 preliminary notions and definitions; for a list of open problems raised by our work refer to Section 7.

2. Preliminary Notions and Definitions

Unless otherwise specified, we consider simple undirected graphs. Let $G = (V, E)$ be such a graph. We denote by n and m the number of vertices and edges of G, respectively. We denote by $d(v)$ the *degree* of a vertex $v \in V$, that is, the number of its incident edges. We say that G has *max-degree* Δ, if G has no vertex with degree larger than Δ, that is, $d(v) \leq \Delta$ for each $v \in V$.

A *drawing* Γ of G is a function that maps each vertex $v \in V$ to a distinct point p_v in $\mathbb{R}^2$, and each edge $(u, v) \in E$ to a simple open Jordan curve connecting p_u and p_v. Drawing Γ is *planar* if no two edges cross. A graph is *planar* if it admits a planar drawing. A planar drawing Γ of G partitions the plane into topologically connected regions, called *faces*; the unbounded face is called *outerface*. A (*topological*) *planar embedding* $\mathcal{E}$ of G is an equivalence class of planar drawings that define the same set of faces. Embedding $\mathcal{E}$ can equivalently be defined by the cyclic orders of the edges incident to each vertex (also called *combinatorial embedding*). For a deeper introduction to graph theoretic basics and to planar graphs, we point the reader to [27] and [1], respectively.

We assume familiarity with standard graph drawing techniques, such as the *canonical ordering* [28, 16] and the *shift-method* by de Fraysseix, Pach and Pollack [28], which we also outline in the following.

The *canonical ordering* for maximal planar graphs [28] is formally defined as follows. Let $G = (V, E)$ be a maximal planar graph and let $\pi = (v_1, \ldots, v_n)$ be a permutation of V. Assume that edges (v_1, v_2), (v_2, v_n) and (v_1, v_n) form a face of G, which we assume w.l.o.g. to be its outerface. For $k = 1, \ldots, n$, let G_k be the subgraph induced by $\cup_{i=1}^{k}\{v_i\}$ and denote by C_k the outerface of G_k. Then, π is a *canonical ordering* of G if for each $k = 2, \ldots, n$ the following hold:

(i) G_k is biconnected,

(ii) all neighbors of v_k in G_{k-1} are (consecutive) on C_{k-1}, and

(iii) If $k \neq n$, then v_k has at least one neighbor v_j, with $j > k$.

A canonical ordering of a maximal planar graph can be computed in linear time [16].

The *shift-method* [28] is a well-known incremental algorithm, which constructs in linear time a planar drawing Γ of a maximal planar graph $G = (V, E)$. Drawing Γ is grid and requires quadratic area. More precisely, based on a canonical order π of G, drawing Γ is constructed as follows. Initially, vertices v_1, v_2 and v_3 are placed at points $(0, 0)$, $(2, 0)$ and $(1, 1)$. For $k = 4, \ldots, n$, assume that a planar drawing Γ_{k-1} of G_{k-1} has been constructed in which each edge of C_{k-1} is drawn as a straight-line segment with slope ± 1, except for the edge (v_1, v_2), which is drawn as a horizontal line segment (*contour condition*; see Figure 2a). Also, assume that each of the vertices $v_1, \ldots, v_{k-1}$ has been associated with a so-called *shift-set*, which for v_1, v_2 and v_3 are singletons containing only themselves. Let $(w_1, \ldots, w_p)$ be the vertices of C_{k-1} from left to right in Γ_{k-1},

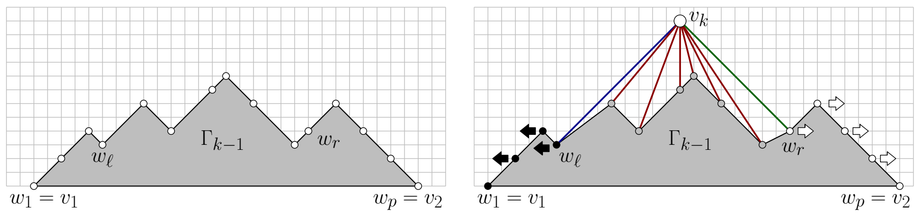

(a) contour condition (b) placement of v_k in Γ_{k-1}

Figure 2: Illustration of the shift-method by de Fraysseix, Pach and Pollack [28].

where $w_1 = v_1$ and $w_p = v_2$. For $i = 1, \ldots, p$, denote by $S(w_i)$ the shift-set of w_i. Let $(w_\ell, \ldots, w_r)$, with $1 \leq \ell < r \leq p$ be the neighbors of v_k from left to right along C_{k-1} in Γ_{k-1}. To avoid edge-overlaps, the algorithm first translates each vertex in $\cup_{i=1}^{\ell} S(w_i)$ one unit to the left and each vertex in $\cup_{i=r}^{p} S(w_i)$ one unit to the right. Then, the algorithm places vertex v_k at the intersection of the line with slope $+1$ through w_ℓ with the line with slope -1 through w_r and sets the shift-set of v_k to $\{v_k\} \cup_{i=\ell+1}^{r-1} S(w_i)$; see Figure 2b.

3. Relationships between Graph Classes

In this section, we consider relationships between the classes of graphs that admit smooth orthogonal k-drawings and octilinear k-drawings, where $k \geq 1$. For the sake of simplicity, we denote these two classes by SC_k and $8C_k$, respectively. Our findings are also summarized in Figure 3.

By definition, $SC_1 \subseteq SC_2$ and $8C_1 \subseteq 8C_2 \subseteq 8C_3$ hold. Since each planar graph of max-degree 8 admits an octilinear 3-drawing [21], class $8C_3$ coincides with the class of planar graphs of max-degree 8. Similarly, class SC_2 coincides with the class of planar graph of max-degree 4, because these graphs admit smooth orthogonal 2-drawings [19]. This also implies that $SC_2 \subseteq 8C_2$, since each planar graph of max-degree 4 admits an octilinear 2-drawing [8]. The relationship $8C_2 \neq 8C_3$ follows from [8], where it was proven that there exist planar graphs of max-degree 6 that do not admit octilinear 2-drawings. The relationship $SC_2 \neq 8C_2$ follows from [24], where it was shown that there exist

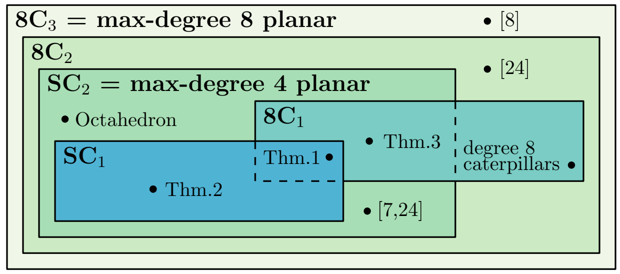

Figure 3: Different inclusion-relationships: For $k \geq 1$, SC_k and $8C_k$ correspond to the classes of graphs that admit smooth orthogonal and octilinear k-drawings, respectively.

planar graphs of max-degree 5 that admit octilinear 2-drawings and no octilinear 1-drawings, and the fact that planar graphs of max-degree 5 cannot be drawn in the smooth orthogonal model. The octahedron graph admits neither a bendless smooth orthogonal drawing [7] nor a bendless octilinear drawing [24]. However, since it is of max-degree 4, it admits 2-drawings in both models [19, 8]. Hence, it belongs to $8C_2 \cap SC_2 \setminus (8C_1 \cup SC_1)$. To prove that $8C_1 \setminus SC_2 \neq \emptyset$, observe that a caterpillar whose spine vertices are of degree 8 clearly admits an octilinear 1-drawing, however, due to its degree it does not admit a smooth orthogonal drawing.

To complete the discussion of the relationships of Figure 3, we have to show that SC_1 and $8C_1$ are incomparable. This is the most interesting part of our proof, since as already mentioned, usually one can "easily" convert a smooth orthogonal drawing of a planar graph of max-degree 4 to a corresponding octilinear one (e.g., by replacing quarter circular arc segments with diagonal edge segments; see Figures 1c-1d for an example), and vice versa. Since the endpoints of each edge of a bendless smooth orthogonal or octilinear drawing are along a line with slope 0, 1, -1 or ∞, such conversions are in principle possible. Two difficulties that might arise are to preserve planarity and to guarantee that no two edges enter a vertex using the same port. Clearly, however, there exist infinitely many (even 4-regular) planar graphs that admit drawings in both models. We formally prove this claim in the following theorem; for an illustration refer to Figure 4.

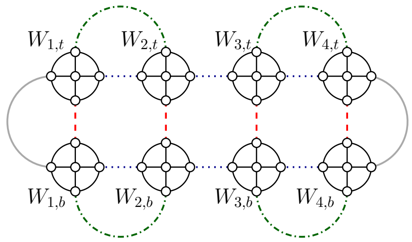

(a) A smooth orthogonal 1-drawing

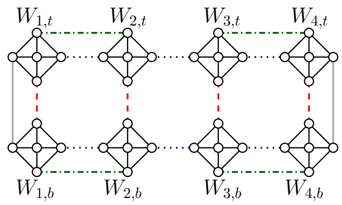

(b) An octilinear 1-drawing

Figure 4: Illustrations for the proof of Theorem 1.

Theorem 1. *There is an infinitely large family of* 4*-regular planar graphs that admit both bendless smooth orthogonal and bendless octilinear drawings.*

Proof. For each $k \in \mathbb{N}_+$ we describe a 4-regular planar graph $G_k = (V_k, E_k)$ with $20k$ vertices that admits both a bendless smooth orthogonal drawing and a bendless octilinear drawing; refer to Figure 4 for the case $k = 2$. Graph G_k has $4k$ subgraphs $W_{i,j}$ such that $1 \leq i \leq 2k$ and $j \in \{t, b\}$, where t and b stand for *top* and *bottom*, respectively. Graph $W_{i,j}$ consists of five vertices $c_{i,j}$, $n_{i,j}$, $w_{i,j}$, $e_{i,j}$, and $s_{i,j}$, such that $W_{i,j}$ is a wheel on five vertices, where $c_{i,j}$ is its center-vertex and cycle $C_{i,j} = (n_{i,j}, w_{i,j}, s_{i,j}, e_{i,j})$ is its rim. Vertices $n_{i,j}$, $w_{i,j}$, $s_{i,j}$ and $e_{i,j}$ are the *north*, *west*, *south* and *east* vertices of $C_{i,j}$, respectively.

All vertices, except for $c_{i,j}$, already have degree three in $W_{i,j}$. So, we only have to describe the edges that make graph G_k 4-regular. For $1 \leq h \leq 2k-1$ and $j \in \{t, b\}$, $(e_{h,j}, w_{h+1,j}) \in E_k$; dotted edges in Figure 4. Also, $(w_{1,t}, w_{1,b}) \in E_k$ and $(e_{2k,t}, e_{2k,b}) \in E_k$; gray edges in Figure 4. For $1 \leq h \leq 2k$, $(s_{h,t}, n_{h,b}) \in E_k$; dashed edges in Figure 4. Finally, for $1 \leq h \leq k$, $(n_{2h-1,t}, n_{2h,t}) \in E_k$ and $(s_{2h-1,b}, s_{2h,b}) \in E_k$; dashed dotted edges in Figure 4. With those additional edges, G_k becomes 4-regular. Figure 4 is a certificate that $G_k = (V_k, E_k)$ indeed admits both a bendless smooth orthogonal drawing and a bendless octilinear drawing, which completes the proof of this theorem. □

To complete the discussion of the inclusion relationships of Figure 3, we show in the next two theorems that SC_1 and $8C_1$ are incomparable.

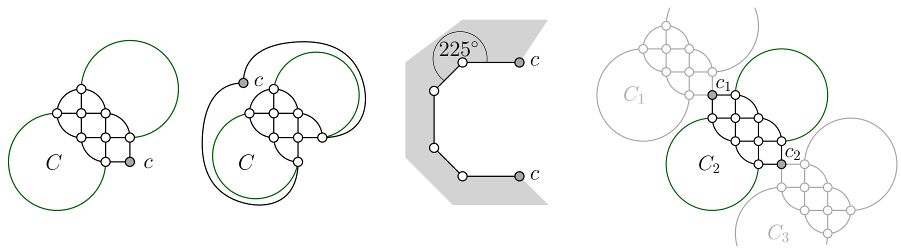

(a) (b) (c) (d)

Figure 5: Illustrations for the proof of Theorem 2.

Theorem 2. *There is an infinitely large family of* 4*-regular planar graphs that admit bendless smooth orthogonal drawings but no bendless octilinear drawing.*

PROOF. Consider the planar graph C of Figure 5a, which is drawn bendless smooth orthogonal. We claim that C admits no bendless octilinear drawing. If one substitutes its degree-2 vertex (denoted by c in Figure 5a) by an edge connecting its two neighbors, then the resulting graph is triconnected, which implies that it admits a unique embedding (up to the choice of its outerface; see Figures 5a-5b). Now, observe that the outerface of any octilinear drawing of graph C (if any) has length at most 5 (Constraint 1). In addition, each vertex of this outerface (except for c, which is of degree 2) must have two ports pointing in the interior of this drawing, because every vertex of C is of degree 4, except for c. This implies that the angle formed by any two consecutive edges of this outerface is at most 225°, except for the pair of edges incident to c (Constraint 2). But if we want to satisfy both constraints, then at least one edge of this outerface must be drawn with a bend; see Figure 5c. Hence, graph C does not admit a bendless octilinear drawing.

Based on graph C, for each $k \in \mathbb{N}_0$ we construct a 4-regular planar graph G_k consisting of $k+2$ biconnected components $C_1, \ldots, C_{k+2}$ arranged in a *chain*; see Figure 5d for the case $k = 1$. Clearly, graph G_k admits a bendless smooth orthogonal drawing for any k. Since components C_1 and C_{k+2} are isomorphic to graph C, graph G_k does not admit a bendless octilinear drawing for any k.□

Theorem 3. *There is an infinitely large family of 4-regular planar graphs that admit bendless octilinear drawings but no bendless smooth orthogonal drawing.*

Proof. Consider the planar graph B of Figure 6a, which is drawn bendless in the octilinear model. First, we discuss some structural properties of graph B. Observe that graph B contains a wheel on five vertices as a subgraph, call it W_5, which is induced by the vertices drawn as circles in Figure 6a. Its center is vertex c (gray colored in Figure 6a) and its rim consists of vertices w_1, w_2, w_3, and w_4. Vertices w_1 and w_2 form a triangular face with vertex t_1; analogously, vertices w_3 and w_4 form a triangular face with t_2 (vertices t_1 and t_2 are drawn as triangles in Figure 6a). Observe that t_1 and t_2 form a separation pair and both are connected to vertices p_1 and p_2 (drawn as pentagons in Figure 6a) forming two pentagonal faces $(p_1, t_1, w_1, w_4, t_2)$ and $(p_2, t_2, w_3, w_2, t_1)$. Observe that p_1 and p_2 also form a separation pair and are both connected to vertices q_1 and q_2 (drawn as squares in Figure 6a) forming two quadrilateral faces (q_1, p_2, t_1, p_1) and (q_2, p_1, t_2, p_2). Hence, B has two separation pairs and two vertices of degree 2 (that is, q_1 and q_2). The remaining vertices of B have degree exactly 4.

Based on graph B, for each $k \in \mathbb{N}_0$ we construct a 4-regular planar graph G_k consisting of $2k+4$ copies of B arranged in a cycle; refer to Figure 6b where each copy of B is drawn as a gray-shaded parallelogram. By construction, graph G_k admits a bendless octilinear drawing, for any k. By planarity, at least one copy of graph B must be embedded with the outerface (p_1, q_1, p_2, q_2) such that each of

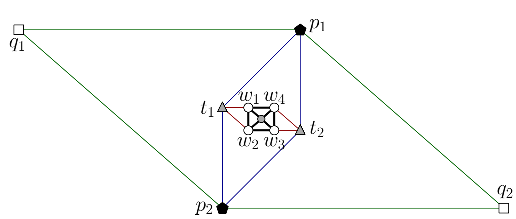

(a)

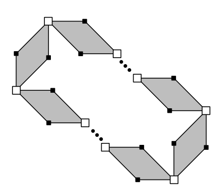

(b)

Figure 6: Illustrations for the proof of Theorem 3.

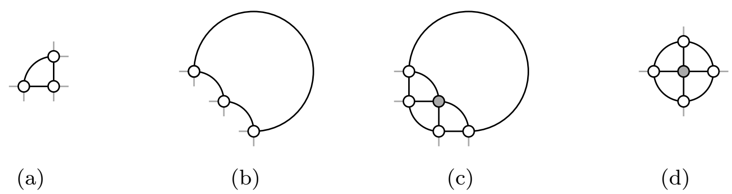

Figure 7: All smooth orthogonal drawings (a)-(b) of a triangular face, and (c)-(d) of a wheel on five vertices, such that all unoccupied ports are on the outerface of the drawing.

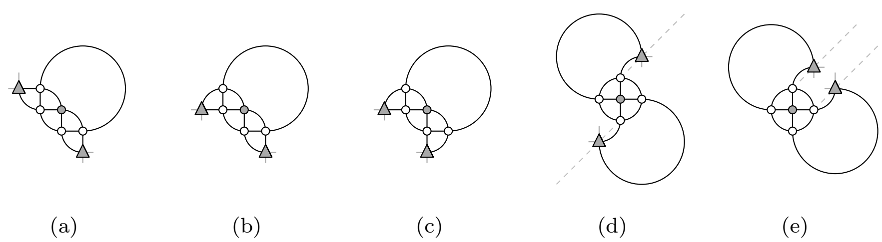

Figure 8: All smooth orthogonal drawings of the subgraph of graph B induced by wheel W_5, and vertices t_1 and t_2, such that all unoccupied ports are on the outerface of the drawing.

q_1 and q_2 has two unoccupied ports incident to this outerface. However, under this restriction the embedding of this particular copy of B must isomorphic to the one of Figure 6a. We now proof that, for any k, graph G_k does not admit a bendless smooth orthogonal drawing by showing that graph B does not admit a bendless smooth orthogonal drawing, when its outerface is (p_1, q_1, p_2, q_2) and each of q_1 and q_2 has two unoccupied ports incident to this outerface.

First, we observe the following: If we want to draw wheel W_5, such that all of its unoccupied ports are on its outerface, then none of its four triangular faces must have an unoccupied port pointing in its interior. In the bendless smooth orthogonal model, there are only two possible drawings for a triangular face fulfilling this property (as shown in [19]), which are illustrated in Figures 7a and 7b. This implies that W_5 admits only two bendless smooth orthogonal drawings such that all of its unoccupied ports are on its outerface, which are illustrated in Figures 7c and 7d.

Next, we consider vertices t_1 and t_2. Since each of them defines a triangular

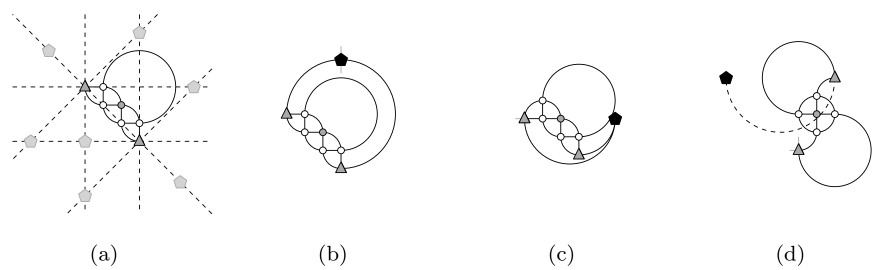

Figure 9: Method used for identifying valid drawings for p_1 and p_2: (a) identification of candidate positions, and (b)-(d) cases of drawings that are not valid.

face in the subgraph induced by wheel W_5, and vertices t_1 and t_2, we can conclude similar as above, that there are five different drawings of this graph, which are illustrated in Figure 8. Note that in Figures 8d and 8e both t_1 and t_2 can independently move along the gray colored diagonal rays.

In the following step, we will consider all candidate positions for placing p_1 and p_2, which we can identify adopting the following simple rule. In a bendless smooth orthogonal drawing, both endpoints of an edge are located along a horizontal, vertical or diagonal line. Both p_1 and p_2 are neighbors of both t_1 and t_2, for which we already defined their locations. If we consider all rays emanating from t_1 and t_2 with slopes $\{0, 1, -1, \infty\}$, then p_1 and p_2 must be located at an intersection of a ray emanating from t_1 and a ray emanating from t_2; in Figure 9a these positions are highlighted as gray pentagons. For each candidate position, we then try to draw the edges from p_1 and p_2 to t_1 and t_2 using one of the edge segments supported by the smooth orthogonal model. The resulting drawing is *valid* if and only if none of the following cases applies:

C.1: a vertex has an unoccupied port that is not incident to the outerface; see Figure 9b,

C.2: a port is used twice; see Figure 9c,

C.3: an edge is involved in crossings; see Figure 9d.

As a result of our analysis, we can conclude that the only valid drawings of

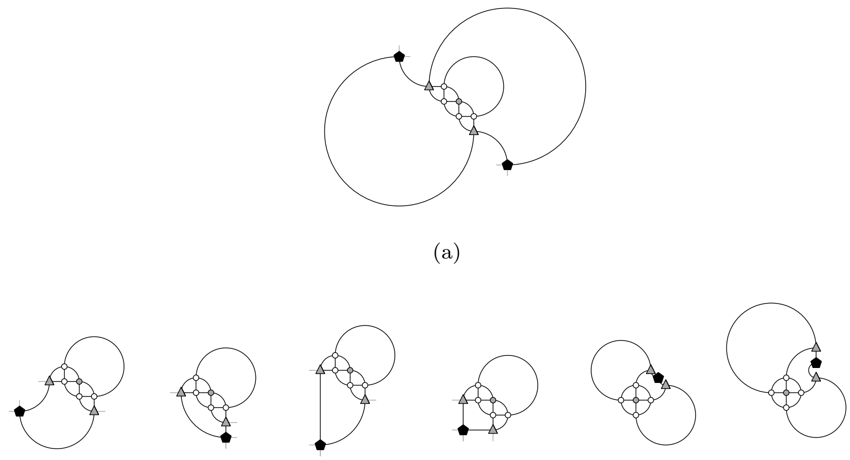

(b) (c) (d) (e) (f) (g)

Figure 10: All valid drawings of the subgraph induced by W_5, t_1, t_2, and at least one of p_1 and p_2.

the subgraph induced by wheel W_5, vertices t_1 and t_2, and at least one of p_1 and p_2 are those shown in Figure 10. Note that in the cases shown in Figures 10b-10g, we can only place one of p_1 and p_2. For the case shown in Figure 10a we proceed by considering all candidate positions of q_1 and q_2, as we did for p_1 and p_2. As a result, we conclude that q_1 and q_2 cannot be added such that each of them has two unoccupied ports on the outerface, which completes the proof of this theorem. □

4. $\mathcal{NP}$-hardness Results

In this section, we study the complexity of the bendless smooth orthogonal and octilinear drawing problems. As a first step towards addressing the complexity of both problems for planar graphs of max-degree 4 in general, here we make an additional assumption. We assume that the input, apart from an embedding, also specifies a *smooth orthogonal* or an *octilinear representation*, which are defined analogously to the orthogonal ones: (i) the angles between consecutive edges incident to a common vertex in the cyclic order around it (given by the planar embedding) are specified, and (ii) the *shape* of each edge (e.g., straight-line, or quarter circular arc) is also specified. In other words, we assume that our input is analogous to the one of the last step of the topology-shape-metrics approach [6]. We first present our reduction for the smooth orthogonal drawing model and afterwards we describe the required modifications for the corresponding reduction for the octilinear model.

Theorem 4. *Given a planar graph G of max-degree 4 and a smooth orthogonal representation $\mathcal{R}$, it is $\mathcal{NP}$-hard to decide whether G admits a bendless smooth orthogonal drawing preserving $\mathcal{R}$. This holds even if $\mathcal{R}$ requires all edges to be drawn as straight-line segments or quarter circular arcs.*

PROOF. Our reduction is from the well-known 3-SAT problem [29]. Given a 3-SAT formula φ in conjunctive normal form, we construct a graph G_φ and a smooth orthogonal representation $\mathcal{R}_\varphi$, such that G_φ admits a bendless smooth orthogonal drawing Γ_φ preserving $\mathcal{R}_\varphi$ if and only if formula φ is satisfiable; for an illustration refer to Figure 11.

The main ideas of our construction are: (i) specific straight-line edges in Γ_φ transport *information* encoded in their length, (ii) rectangular faces of Γ_φ propagate the edge length of one side to its opposite side, and (iii) for a face composed of two straight-line edges and a quarter circular arc, the straight-line edges are of same length, which allows us to change the *direction* in which the information "flows".

Variable gadget. For each variable x of φ, we introduce a gadget, which is illustrated in Figure 12. The bold-drawn quarter circular arc ensures that the sum of the edge lengths to its left is the same as the sum of the edge lengths to its bottom (refer to the edges with gray endvertices). As "input" the gadget gets three edges of unit length $\ell(u)$. This ensures that $\ell(x) + \ell(\overline{x}) = 3 \cdot \ell(u)$ holds for the "output literals" x and $\overline{x}$, where $\ell(x)$ and $\ell(\overline{x})$ denote the lengths of two edges representing x and $\overline{x}$.

To introduce our concept, assume that the lengths of all straight-line edges are integral and at least 1. If we could require $\ell(u) = 1$, then $\ell(x), \ell(\overline{x}) \in \{1, 2\}$.

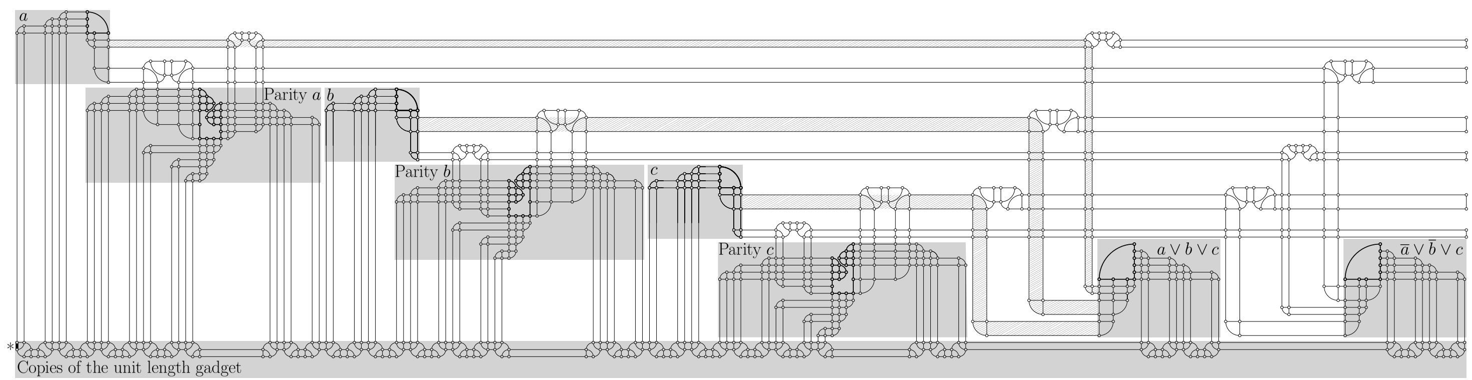

Figure 11: Drawing Γ_φ for $\varphi = (a \vee b \vee c) \wedge (\overline{a} \vee \overline{b} \vee c)$ and the assignment $a =$ `false` and $b = c =$ `true`.

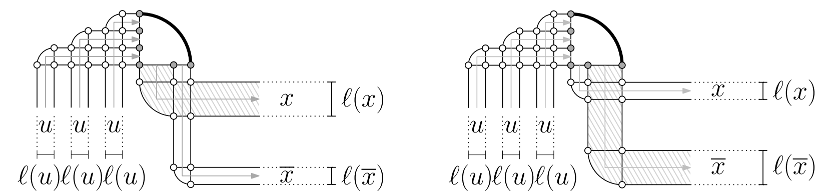

(a) true state: $\ell(x) = 2$, $\ell(\overline{x}) = 1$ (b) false state: $\ell(x) = 1$, $\ell(\overline{x}) = 2$

Figure 12: The variable gadget; gray-colored arrows show the information "flow".

This would allow us to encode the assignment $x = \texttt{true}$ with $\ell(x) = 2$ and $\ell(\overline{x}) = 1$, and the assignment $x = \texttt{false}$ with $\ell(x) = 1$ and $\ell(\overline{x}) = 2$ (i.e., a length of 2 implies that the literal is true). However, if we cannot avoid, e.g., that $\ell(u) = 2$, then the variable gadget would not prevent us from setting $\ell(x) = \ell(\overline{x}) = 3$, which means that x and $\overline{x}$ are "half-true". We solve this issue by introducing the so-called *parity gadget*, that allows us to relax the integer constraint and to ensure that $\ell(x), \ell(\overline{x}) \in \{\ell(u) + \varepsilon,\ 2\ell(u) - \varepsilon\}$, for $\varepsilon << \ell(u)$.

Parity gadget. For each variable x of φ, graph G_φ has a gadget, which results in overlaps in Γ_φ, if the values of $\ell(x)$ and $\ell(\overline{x})$ do not differ significantly. For an illustration, refer to Figure 13. The central part of this gadget is a "*vertical gap*" of width $3 \cdot \ell(u)$ (shaded in gray in Figures 13a-13c) with two blocks of vertices (triangular- and square-shaped in Figures 13a-13c) pointing inside the gap; a more detailed illustration of the vertical gap is given in Figure 13d. Each block defines two square-shaped faces and three triangular faces, each formed by two straight-line edges and a quarter circular arc. Depending on the choice of $\ell(x)$ and $\ell(\overline{x})$, one of the blocks may be located above the other. If $\ell(x) \approx \ell(\overline{x})$, however, we can observe that the two blocks are not far enough apart from each other, which leads to overlaps, as illustrated in Figure 13c.

Refer to Figure 13d. Consider the case where $x = \texttt{false}$. The case where $x = \texttt{true}$ is symmetric. If $x = \texttt{false}$, we have to ensure that the two quarter circular arcs that are intersected by the dashed diagonal line-segment of Figure 13d do not introduce crossings, i.e., in other words the top one should be located on top

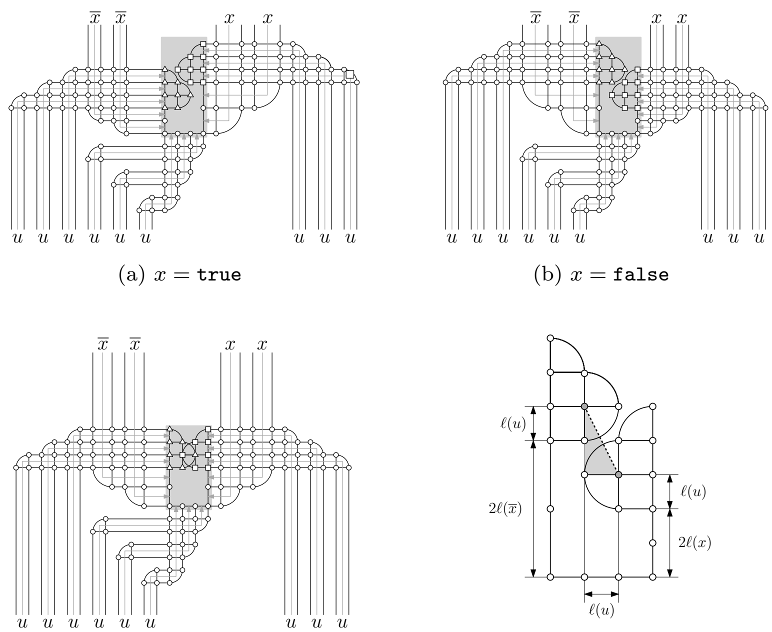

(a) $x =$ `true` (b) $x =$ `false`

(c) $\ell(x) \approx \ell(\overline{x})$ (d) Detail

Figure 13: The parity gadget; gray-colored arrows show the information "flow".

of the bottom one in Figure 13d. Since we know that both of these arcs have radius $\ell(u)$, their centers (gray-colored in Figure 13d) should be at a distance grater than $2 \cdot \ell(u)$ apart from each other, i.e., the length of the dashed diagonal line segment is at least $2 \cdot \ell(u)$. However, the length of this segment can be easily expressed in dependence of $\lambda = \ell(\overline{x}) - \ell(x)$ as follows: $\sqrt{4\lambda^2 + \ell(u)^2}$. Hence, in order to avoid crossings it is not difficult to see that $\lambda > \sqrt{3}/2 \cdot \ell(u) \approx 0.866 \cdot \ell(u)$. This implies that $\ell(x), \ell(\overline{x}) \in (0,\ 1.067 \cdot \ell(u)) \cup (1.933 \cdot \ell(u),\ 3)$, i.e., $\varepsilon < 0.067 \cdot \ell(u)$ in order to avoid crossings.

Clause gadget. For each clause of φ with literals a, b and c, we introduce a gadget, which is illustrated in Figure 14. The bold-drawn quarter circular arc of Figure 14 compares two sums of information. From the righthand side, four edges of unit length "enter" the arc. Observe that there is also a *free edge* (marked with an asterisk in Figure 14), which also contributes to the sum but

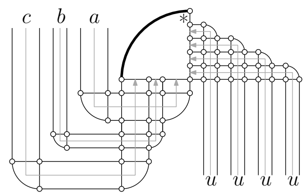

Figure 14: Clause gadget; gray-colored arrows show the information “flow”.

(a) crossing gadget (b) copy gadget

Figure 15: Auxiliary gadgets; gray-colored arrows show the information “flow”.

can be stretched independently of any other edge. Hence, the sum of edge lengths on the righthand side of this arc is greater than $4 \cdot \ell(u)$. The three literals “enter” at the bottom; the sum here is $\ell(a) + \ell(b) + \ell(c)$. Combining both, we obtain that $\ell(a) + \ell(b) + \ell(c) > 4 \cdot \ell(u)$ must hold. This implies that not all a, b and c can be `false`, since in this case $\ell(a) + \ell(b) + \ell(c) = 3 \cdot (\ell(u) + \varepsilon) < 4 \cdot \ell(u)$, because $\varepsilon << \ell(u)$. However, if at least one literal is `true`, then $\ell(a) + \ell(b) + \ell(c) \geq 4 \cdot \ell(u) + \varepsilon$ and the aforementioned inequality holds.

Auxiliary gadgets. The *crossing gadget* just consists of a rectangle and is used to allow two flows of information to cross each other; see Figure 15a. The *copy gadget* takes an information and creates three copies of this information; see Figure 15b. This is because the vertices of each gray colored quadrilateral face in Figure 15b must be located at the corners of a rectangle whose sides have slopes ± 1, which implies that its opposite sides must be of the same length. Finally, the *unit length gadget* is a single edge, which we assume to have length $\ell(u)$. In Figure 11, the unit length gadget is marked with an asterisk and is copied several times using multiple copies of the copy gadget (all of which lie in the gray colored box in the bottom part of the figure).

Description of the construction. We now describe our construction; see Figure 11. Graph G_φ contains one unit length gadget, which is copied multiple times using the copy gadget (the number of copies depends linearly on the number of variables ν and clauses μ of φ). For each variable of φ, graph G_φ has a variable gadget and a parity gadget, each of which is connected to different copies of the unit length gadget. For each clause of φ, graph G_φ has a clause gadget, which has four connections to different copies of the unit length gadget. We compute $\mathcal{R}_\varphi$ as follows. We place the variable gadget of each variable x above and to the left of its parity gadget and we connect the output literals of the variable gadget of x with its parity gadget through a copy gadget. We place the variable and the parity gadgets of the i-th variable below and to the right of the corresponding ones of the $(i-1)$-th variable. We place each clause gadget to the right of the sketch constructed so far, so that the gadget of the i-th clause is to the right of the $(i-1)$-th clause. This allows us to connect copies of the output literals of the variable gadget of each variable with the clause gadgets that contain it, so that all possible crossings (which are resolved using the crossing gadget) appear above the clause gadgets. More precisely, if a clause contains a literal of the i-th variable, we have a crossing with the literals of all variables with indices $(i+1)$ to ν. Hence, for each clause we add $O(\nu)$ crossings and three copy gadgets. Note that all copy gadgets of the unit length gadget lie below all variable, parity, and clause gadgets. The obtained representation $\mathcal{R}_\varphi$ conforms with the one of Figure 11. The construction can be done in $O(\nu\mu)$ time.

To complete the proof, assume that graph G_φ admits a bendless smooth orthogonal drawing Γ_φ preserving $\mathcal{R}_\varphi$. We compute a truth assignment for φ as follows. For each variable x of φ, we set x to `true` if and only if $\ell(x) \geq 1.933 \cdot \ell(u)$. Since for each clause $(a \vee b \vee c)$ of φ we have that $\ell(a) + \ell(b) + \ell(c) > 4 \cdot \ell(u)$, it follows that at least one of a, b and c must be `true`. Hence, φ admits a truth assignment. For the opposite direction, based on a truth assignment of φ, we can set, e.g., $\ell(x) = 1.95$ and $\ell(\overline{x}) = 1.05$ for each variable x, assuming that $\ell(u) = 1$. Then, arranging the variable and the clause gadgets of G_φ as in Figure 11 yields a bendless smooth orthogonal drawing Γ_φ preserving $\mathcal{R}_\varphi$. $\square$

Remark 1. The special case of our problem, in which circular arcs are not present, is known as *HV-rectilinear planarity testing* [30]. As opposed to our problem, HV-rectilinear planarity testing is polynomial-time solvable in the fixed embedding setting [31] (and becomes $\mathcal{NP}$-hard in the variable embedding setting [32]). It turns out, however, that in the presence of quarter circular arcs the problem becomes $\mathcal{NP}$-hard.

We now proceed to prove the analogous of Theorem 4 for the octilinear model.

Theorem 5. *Given a planar graph G of max-degree 4 and an octilinear representation $\mathcal{R}$, it is $\mathcal{NP}$-hard to decide whether G admits a bendless octilinear drawing preserving $\mathcal{R}$.*

Proof. In principle, our proof follows the same reduction scheme as the one of Theorem 4. More precisely, we can adjust to the octilinear model by replacing quarter circular arcs with diagonal segments. By doing so, we maintain planarity (by construction). However, the parity gadget has to be adjusted properly, so to maintain its functionality. To this end, we only change the vertical gap of parity gadget as in Figure 16, which shows the case where $x =$ `false`; the case where $x =$ `true` is symmetric.

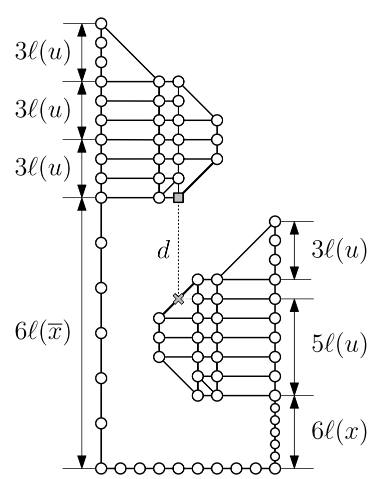

Figure 16: The parity gadget for the octilinear model.

It is not difficult to see that the smallest vertical distance d between the blocks in the vertical gap (illustrated as a dotted line-segment in Figure 16) equals to $6\ell(\overline{x}) - 6\ell(x) - 5\ell(u)$, which implies $\ell(\overline{x}) - \ell(x) > 5/6 \cdot \ell(u)$, since d must be strictly greater than zero. Thus, $\varepsilon < 0.084 \cdot \ell(u) << \ell(u)$. $\square$

5. Bi-Monotone Drawings

In this section, we study variants of the *Kandinsky* drawing model [4, 25, 26], which forms an extension of the orthogonal model to graphs of degree greater than 4. In this model, the vertices are represented as squares, placed on a *coarse grid* with multiple edges attached to each side of them aligned on a *finer grid*. Since Kandinsky drawings find applications in several area, such as VLSI design, UML diagrams and business process modeling, this drawing model has been extensively studied over the years; see, e.g., [33, 34].

The Kandinsky model allows for natural extensions to both smooth orthogonal and octilinear models. We are aware of only one preliminary result in this direction for the former model: A linear time drawing algorithm is presented in [7] for the production of smooth orthogonal 2-drawings for planar graphs of arbitrary degree in quadratic area, in which all vertices are on a line ℓ and the edges are drawn either as half circles (above or below ℓ), or as two consecutive half circles one above and one below ℓ (that is, the latter ones are of complexity 2, but they are at most $\lfloor (n-3)/2 \rfloor$ [35]).

For an input maximal planar graph G (of arbitrary degree), our goal is to construct a smooth orthogonal (or an octilinear) 2-drawing for G with the following aesthetic benefits over the aforementioned drawing algorithm:

(i) the vertices are distributed evenly over the drawing area, and

(ii) each edge is *bi-monotone* [36], i.e., xy-monotone.

We achieve our goal at the cost of slightly more edges drawn with complexity 2 or at the cost of increased drawing area (but still polynomial).

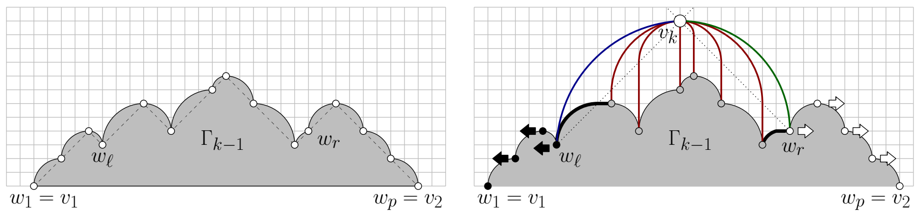

(a) contour condition (b) placement of v_k in Γ_{k-1}

Figure 17: Illustration of the modified shift-method for the smooth orthogonal model.

Our first approach is a modification of the *shift-method* [28] (see also Section 2). Based on a canonical order $\pi = (v_1, \ldots, v_n)$ of G, we construct a planar smooth orthogonal 2-drawing Γ of G in the Kandinsky model, as follows. We place v_1, v_2 and v_3 at points $(0, 0)$, $(2, 0)$ and $(1, 1)$, respectively. Hence, we can draw edge (v_1, v_2) as a horizontal line-segment, and each of edges (v_1, v_3) and (v_2, v_3) as a quarter circular arc. We also color edge (v_1, v_3) blue and edge (v_2, v_3) green. For $k = 4, \ldots, n$, assume that a smooth orthogonal 2-drawing Γ_{k-1} of the subgraph G_{k-1} of G induced by $v_1, \ldots, v_{k-1}$ has been constructed, in which each edge of the outerface C_{k-1} of Γ_{k-1} is drawn as a quarter circular arc, whose endvertices are on a line with slope ± 1, except for edge (v_1, v_2), which is drawn as a horizontal segment (called *contour condition* in the shift-method). For an illustration, refer to Figure 17a. Each of $v_1, \ldots, v_{k-1}$ is also associated with a so-called *shift-set*, which for v_1, v_2 and v_3 are singletons containing only themselves (as in the shift-method).

Let $(w_1, \ldots, w_p)$ be the vertices of C_{k-1} from left to right in Γ_{k-1}, where $w_1 = v_1$ and $w_p = v_2$. Let $(w_\ell, \ldots, w_r)$, $1 \leq \ell < r \leq p$, be the neighbors of v_k from left to right along C_{k-1} in Γ_{k-1}. As in the shift-method, our algorithm first translates each vertex in $\cup_{i=1}^{\ell} S(w_i)$ one unit to the left and each vertex in $\cup_{i=r}^{p} S(w_i)$ one unit to the right, where $S(v)$ is the shift-set of $v \in V$. During this translation, each of edges $(w_\ell, w_{\ell+1})$ and (w_{r-1}, w_r) acquires a horizontal segment (see the bold edges of Figure 17b). We place vertex v_k at the intersection of line λ_ℓ with slope $+1$ through w_ℓ with line λ_r with slope -1 through

w_r (which are drawn dotted in Figure 17b) and we set the shift-set of v_k to $\{v_k\} \cup_{i=\ell+1}^{r-1} S(w_i)$, as in the shift-method. We draw each of edges (w_ℓ, v_k) and (v_k, w_r) as a quarter circular arc. The remaining edges incident to v_k are drawn with complexity 2. More precisely, for $i = \ell+1, \ldots, r-1$, edge (w_i, v_k) has a vertical line-segment that starts from w_i and ends either at λ_ℓ or λ_r and a quarter circular arc from the end of the previous segment to v_k. Hence, the contour condition is satisfied.

We color edge (w_ℓ, v_k) blue, edge (v_k, w_r) green and the remaining edges incident to v_k in G_k red (this type of coloring is also known as *Schnyder coloring* [37, 38]). Observe that each blue and green edge consists of a quarter circular arc and a horizontal segment (that may have zero length), while a red edge consists of a vertical segment and a quarter circular arc (that may have zero radius). We are now ready to state the following theorem.

Theorem 6. *A maximal planar n-vertex graph admits a bi-monotone planar smooth orthogonal 2-drawing in the Kandinsky model, which requires $O(n^2)$ area and can be computed in $O(n)$ time.*

Proof. Bi-monotonicity and the fact that the computed drawing is a 2-drawing follows by construction. The time complexity follows from [39]. Planarity is proven by induction. Drawing Γ_3 is planar by construction. Assuming that Γ_{k-1} is planar, we observe that no two edges incident to v_k cross in Γ_k. Also, these edges do not cross edges of Γ_{k-1}. Since the radii of the arcs of the edges incident to vertices that are shifted remain unchanged and since edges incident to vertices in the shift-sets retain their shape, drawing Γ_k is planar. This completes our proof. □

For the octilinear model, we can analogously state the following theorem.

Theorem 7. *A maximal planar n-vertex graph admits a bi-monotone planar octilinear 2-drawing in the Kandinsky model, which requires $O(n^2)$ area and can be computed in $O(n)$ time. Additionally, each bend is at $135°$.*

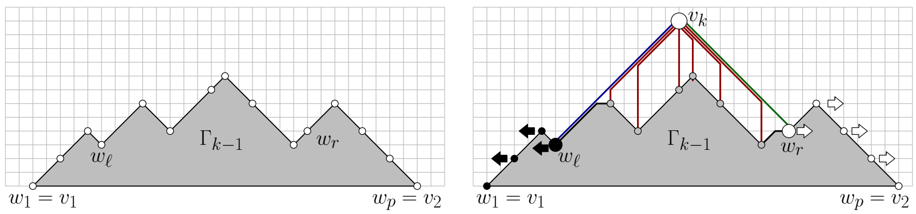

(a) contour condition (b) placement of v_k in Γ_{k-1}

Figure 18: Illustration of the modified shift-method for the octilinear model.

Proof. The proof is rather simple. We can actually convert the layout computed for the smooth orthogonal model to octilinear by redrawing all its quarter circular arcs to diagonal segments; see also Figure 18b. This results in bends at 135°. Planarity follows from the fact that the blue and the green edges do not pass through vertices by virtue of construction. □

We reduce the number of edges drawn with complexity 2, by computing new y-coordinates for the vertices, while keeping their x-coordinates unchanged. To achieve this, we process the vertices of G in the same canonical ordering $\pi = (v_1, \ldots, v_n)$ maintaining the following invariant (which is a modification of the contour condition):

(I.1) Each edge of the outerface has a quarter circular arc segment of non-zero radius, except for the edge (v_1, v_2); see Figure 19a.

Initially, we set $y(v_1) = y(v_2) = 0$. For $k = 3, \ldots, n$, we assume as in the shift-method that the neighbors of vertex v_k in Γ_{k-1} are $(w_\ell, \ldots, w_r)$ from left to right along C_{k-1}. Next, from each of the vertices $w_\ell, \ldots, w_r$ that are strictly to the left (right) of v_k, we draw a line with slope $+1$ (-1, resp.); refer to the dashed drawn lines of Figure 19b. The intersections of these lines with the vertical line $L_k : x = x(v_k)$ are *candidate positions* for the placement of v_k. If there is a vertex w_i, for some $i = \ell, \ldots, r$, whose x-coordinate is equal to the x-coordinate of vertex v_k (that is, $x(w_i) = x(v_k)$), then there is one more candidate position, called *trivial*, for the placement of v_k, which is also along

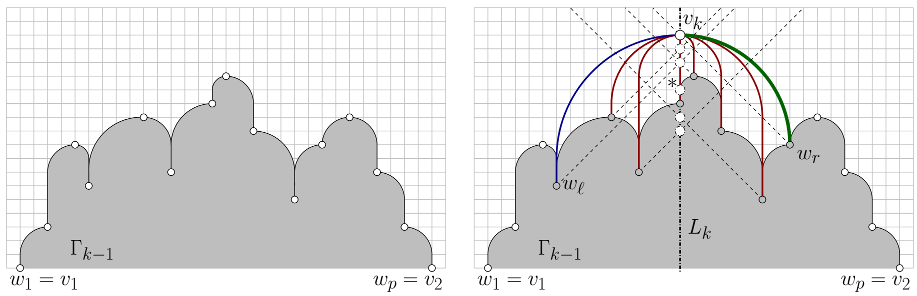

(a) invariant (I.1)

(b) placement of v_k in Γ_{k-1}

Figure 19: Illustration of the contour condition and placement of v_k in Γ_{k-1}.

the line L_k at $(x(w_i), y(w_i)+1)$; refer to the candidate position marked with an asterisk in Figure 19b. We choose to place v_k at the highest candidate position. Formally, the y-coordinate of vertex v_k is computed as follows:

$$y(v_k) = \max_{w \in \{w_\ell, \dots, w_r\}} \{y(w) + \max\{\Delta_x(v_k, w), 1\}\} \tag{1}$$

Let $w^* \in \{w_\ell, \dots, w_r\}$ be the vertex of C_{k-1} defining the highest candidate position. Note that, in general, more than one vertex may define the highest candidate position. It is not difficult to see that edge (v_k, w^*) can be drawn as a quarter circular arc, unless v_k is placed in the trivial candidate position, in which case we draw it as a vertical line-segment of unit length. This immediately implies that (at least) $n-1$ edges are drawn with complexity 1, as desired. We draw the remaining edges incident to v_k with complexity 2. More precisely, each of these edges is composed of two segments; one quarter circular arc segment incident to v_k followed by a vertical line-segment incident to the other endpoint. Since $x(w_\ell) < x(v_k) < x(w_r)$, it follows that Invariant (I.1) is maintained, by construction; in addition, note that the quarter circular arc of Invariant (I.1) is always incident to vertex v_k. We are now ready to state the following theorem.

Theorem 8. *A maximal planar n-vertex graph G admits a bi-monotone planar smooth orthogonal 2-drawing Γ with at least $n-1$ edges drawn with complexity 1 in the Kandinsky model, which requires $O(n^3)$ area and can be computed in $O(n)$ time.*

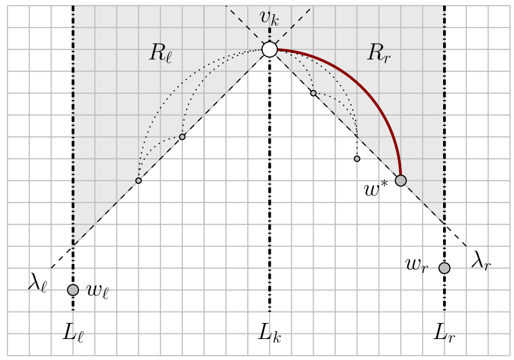

Figure 20: Illustration for the proof of Theorem 8.

PROOF. The time complexity follows from the shift-method. Since the fact that at least $n-1$ edges are drawn with complexity 1 has already been discussed, in order to prove this theorem, it remains to show that the computed drawing is planar and that its area is cubic. The latter can be proven immediately. Since the horizontal distance between any two vertices of G in Γ is $O(n)$, it follows that the vertical distance between any two consecutive (in the canonical ordering) vertices in Γ cannot be more than $O(n)$, which implies that the height of Γ is at most $O(n^2)$. Hence, the area occupied by Γ is $O(n^3)$.

We prove planarity inductively. For the base of the induction, note that drawing Γ_3 is planar. Assuming that Γ_{k-1} is planar, we show in the following that Γ_k is planar, as well. By construction, the edges that are incident to v_k do not cross each other. This is because of Invariant (I.1), which ensures that no two neighbors of v_k in G_k have the same x-coordinate. Since drawing Γ_{k-1} remains unchanged after placing v_k (and hence planar as subdrawing of Γ_k), it remains to prove that the edges incident to v_k do not introduce crossings with edges of Γ_{k-1}; in particular with edges of C_{k-1}.

Let L_ℓ and L_r be the vertical lines through w_ℓ and w_r in Γ_k, respectively; see Figure 20. By construction, there is no vertex in the region R_ℓ between L_ℓ and L_k that lies above the line λ_ℓ with slope $+1$ through v_k. Symmetrically, there is no vertex in the region R_r between L_k and L_r that lies above the line λ_r with slope -1 through v_k; both regions R_ℓ and R_r are highlighted in gray in

Figure 20. However, along the parts of λ_ℓ and λ_r that lie in the interior of R_ℓ and R_r, respectively, there might exist several vertices (one of them is w^*).

Since w_ℓ and w_r are the leftmost and rightmost neighbors of v_k in Γ_{k-1}, it follows that the neighbors $w_\ell, \ldots, w_r$ of v_k in G_k lie between L_ℓ and L_r (and either completely below or along λ_ℓ and λ_r). Each edge incident to v_k in G_k has a circular arc segment that starts from v_k and ends at a point along λ_ℓ or λ_r (followed by a vertical segment of possibly zero length towards one of $w_\ell, \ldots, w_r$), such that no two such circular arc segments overlap, as by Invariant (I.1) no two vertices among $w_\ell, \ldots, w_r$ have the same x-coordinate. Since in regions R_ℓ and R_r there are no vertices of G_k, it follows that these circular arcs may only cross other circular arc segments that lie in R_ℓ and R_r, which must have both endpoints either along λ_ℓ or along λ_r. However, such crossings are not possible because the radius of the circular arc segment of an edge (w_i, w_{i+1}) of C_{k-1} is smaller than the radius of the circular arc segments of both edges (v_k, w_i) and (v_k, w_{i+1}) in such a scenario; refer to the dotted drawn edges of Figure 20. Since the vertical edge segments incident to each of $w_\ell, \ldots, w_r$ neither cross each other nor cross edges of C_{k-1}, it follows that Γ_k is in fact planar. $\square$

6. Example Run of our Drawing Algorithm

In this section, we describe an example run of our drawing algorithm from Section 5 on the octahedron graph, which is a triangulated 4-regular planar graph on six vertices. Figure 21 shows the steps of constructing a smooth orthogonal drawing of this graph using our modification of the shift-method.

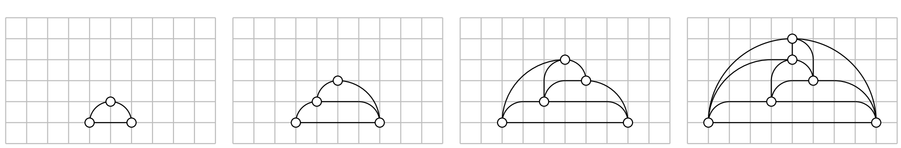

(a) (b) (c) (d)

Figure 21: The steps of drawing the octahedron graph with our modified shift-method.

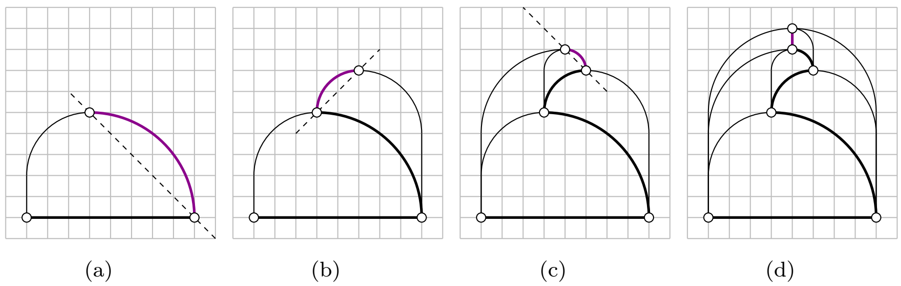

Figure 22: Illustration of the reduction of the number of edges drawn with complexity 2.

Figure 22 illustrates how new y-coordinates are assigned to the vertices so to reduce the number of edges drawn with complexity 2 (observe that the x-coordinates are the ones of Figure 21d). In particular, Figure 22a shows how this is done for the first three vertices. Figures 22b, 22c and 22d illustrate how the fourth, the fifth and the sixth vertex of the octahedron graph is added. The bold edges in each subfigure of Figure 22 are the ones defining drawn with complexity 1 at each step of the canonical order. The final drawing is the one of Figure 22d. We emphasize on the additional area consumption, which on the vertical dimension increases to quadratic.

7. Conclusions

In this paper, we continued the study on smooth orthogonal and octilinear drawings. Our $\mathcal{NP}$-hardness proofs are a first step towards settling the complexity of both drawing problems. We conjecture that deciding whether a planar graph admits a bendless smooth orthogonal drawing is $\mathcal{NP}$-hard, even in the case where only the planar embedding is specified by the input. For the octilinear drawing problem, it is of interest to know if it remains $\mathcal{NP}$-hard even for planar graphs of max-degree 4 or if these graphs allow for a decision algorithm. Our drawing algorithms guarantee bi-monotone 2-drawings with a certain number of complexity-1 edges for maximal planar graphs. Improvements or generalizations to non-triangulated planar graphs are of importance.

Acknowledgements. This work has been supported by DFG grant Ka812/17-1. The authors would like to thank Patrizio Angelini and Martin Gronemann for useful discussions.

References

[1] G. Di Battista, P. Eades, R. Tamassia, I. G. Tollis, Graph Drawing: Algorithms for the Visualization of Graphs, Prentice-Hall, 1999.

[2] M. Kaufmann, D. Wagner (Eds.), Drawing Graphs, Methods and Models, Vol. 2025 of LNCS, Springer, 2001. `doi:10.1007/3-540-44969-8`.

[3] T. C. Biedl, G. Kant, A better heuristic for orthogonal graph drawings, Comput. Geom. 9 (3) (1998) 159–180. `doi:10.1016/S0925-7721(97)00026-6`.

[4] U. Fößmeier, M. Kaufmann, Drawing high degree graphs with low bend numbers, in: F. Brandenburg (Ed.), Graph Drawing, Vol. 1027 of LNCS, Springer, 1995, pp. 254–266. `doi:10.1007/BFb0021809`.

[5] Y. Liu, A. Morgana, B. Simeone, A linear algorithm for 2-bend embeddings of planar graphs in the two-dimensional grid, Discrete Applied Mathematics 81 (1-3) (1998) 69–91. `doi:10.1016/S0166-218X(97)00076-0`.

[6] R. Tamassia, On embedding a graph in the grid with the minimum number of bends, SIAM J. Comput. 16 (3) (1987) 421–444. `doi:10.1137/0216030`.

[7] M. A. Bekos, M. Kaufmann, S. G. Kobourov, A. Symvonis, Smooth orthogonal layouts, J. Graph Algorithms Appl. 17 (5) (2013) 575–595. `doi:10.7155/jgaa.00305`.

[8] M. A. Bekos, M. Gronemann, M. Kaufmann, R. Krug, Planar octilinear drawings with one bend per edge, J. Graph Algorithms Appl. 19 (2) (2015) 657–680. `doi:10.7155/jgaa.00369`.

[9] C. A. Duncan, D. Eppstein, M. T. Goodrich, S. G. Kobourov, M. Nöllenburg, Lombardi drawings of graphs, J. Graph Algorithms Appl. 16 (1) (2012) 85–108. doi:10.7155/jgaa.00251.

[10] D. Eppstein, Planar lombardi drawings for subcubic graphs, in: W. Didimo, M. Patrignani (Eds.), Graph Drawing, Vol. 7704 of LNCS, Springer, 2012, pp. 126–137. doi:10.1007/978-3-642-36763-2_12.

[11] S. Hong, D. Merrick, H. A. D. do Nascimento, Automatic visualisation of metro maps, J. Vis. Lang. Comput. 17 (3) (2006) 203–224. doi:10.1016/j.jvlc.2005.09.001.

[12] M. Nöllenburg, Automated drawing of metro maps, Master's thesis, Fakultät für Informatik, Universität Karlsruhe (TH) (Aug. 2005).

[13] M. Nöllenburg, A. Wolff, Drawing and labeling high-quality metro maps by mixed-integer programming, IEEE Trans. Vis. Comput. Graph. 17 (5) (2011) 626–641. doi:10.1109/TVCG.2010.81.

[14] J. M. Stott, P. Rodgers, J. C. Martinez-Ovando, S. G. Walker, Automatic metro map layout using multicriteria optimization, IEEE Trans. Vis. Comput. Graph. 17 (1) (2011) 101–114. doi:10.1109/TVCG.2010.24.

[15] R. Tamassia (Ed.), Handbook on Graph Drawing and Visualization, Chapman and Hall/CRC, 2013.

[16] G. Kant, Drawing planar graphs using the canonical ordering, Algorithmica 16 (1) (1996) 4–32. doi:10.1007/BF02086606.

[17] A. Garg, R. Tamassia, On the computational complexity of upward and rectilinear planarity testing, SIAM J. Comput. 31 (2) (2001) 601–625. doi:10.1137/S0097539794277123.

[18] C. A. Duncan, M. T. Goodrich, Planar orthogonal and polyline drawing algorithms, in: R. Tamassia (Ed.), Handbook on Graph Drawing and Visualization., Chapman and Hall/CRC, 2013, pp. 223–246.

[19] M. J. Alam, M. A. Bekos, M. Kaufmann, P. Kindermann, S. G. Kobourov, A. Wolff, Smooth orthogonal drawings of planar graphs, in: A. Pardo, A. Viola (Eds.), LATIN, Vol. 8392 of LNCS, Springer, 2014, pp. 144–155. `doi:10.1007/978-3-642-54423-1_13`.

[20] M. A. Bekos, M. Gronemann, S. Pupyrev, C. N. Raftopoulou, Perfect smooth orthogonal drawings, in: N. G. Bourbakis, G. A. Tsihrintzis, M. Virvou (Eds.), IISA, IEEE, 2014, pp. 76–81. `doi:10.1109/IISA.2014.6878731`.

[21] B. Keszegh, J. Pach, D. Pálvölgyi, Drawing planar graphs of bounded degree with few slopes, SIAM J. Discrete Math. 27 (2) (2013) 1171–1183. `doi:10.1137/100815001`.

[22] G. Kant, Hexagonal grid drawings, in: E. W. Mayr (Ed.), WG, Vol. 657 of LNCS, Springer, 1992, pp. 263–276. `doi:10.1007/3-540-56402-0_53`.

[23] E. D. Giacomo, G. Liotta, F. Montecchiani, The planar slope number of subcubic graphs, in: A. Pardo, A. Viola (Eds.), LATIN, Vol. 8392 of LNCS, Springer, 2014, pp. 132–143. `doi:10.1007/978-3-642-54423-1_12`.

[24] M. A. Bekos, M. Kaufmann, R. Krug, On the total number of bends for planar octilinear drawings, J. Graph Algorithms Appl. 21 (4) (2017) 709–730. `doi:10.7155/jgaa.00436`.

[25] P. Bertolazzi, G. Di Battista, W. Didimo, Computing orthogonal drawings with the minimum number of bends, IEEE Trans. Computers 49 (8) (2000) 826–840. `doi:10.1109/12.868028`.

[26] G. Di Battista, W. Didimo, M. Patrignani, M. Pizzonia, Orthogonal and quasi-upward drawings with vertices of prescribed size, in: J. Kratochvíl (Ed.), Graph Drawing, Vol. 1731 of LNCS, Springer, 1999, pp. 297–310. `doi:10.1007/3-540-46648-7_31`.

[27] F. Harary, Graph theory, Addison-Wesley, 1991.

[28] H. de Fraysseix, J. Pach, R. Pollack, How to draw a planar graph on a grid, Combinatorica 10 (1) (1990) 41–51. doi:10.1007/BF02122694.

[29] M. R. Garey, D. S. Johnson, Computers and Intractability: A Guide to the Theory of NP-Completeness, W. H. Freeman, 1979.

[30] J. Manuch, M. Patterson, S. Poon, C. Thachuk, Complexity of finding non-planar rectilinear drawings of graphs, in: U. Brandes, S. Cornelsen (Eds.), Graph Drawing, Vol. 6502 of LNCS, Springer, 2010, pp. 305–316. doi:10.1007/978-3-642-18469-7_28.

[31] S. Durocher, S. Felsner, S. Mehrabi, D. Mondal, Drawing hv-restricted planar graphs, in: A. Pardo, A. Viola (Eds.), LATIN, Vol. 8392 of LNCS, Springer, 2014, pp. 156–167. doi:10.1007/978-3-642-54423-1_14.

[32] W. Didimo, G. Liotta, M. Patrignani, On the complexity of hv-rectilinear planarity testing, in: C. A. Duncan, A. Symvonis (Eds.), Graph Drawing, Vol. 8871 of LNCS, Springer, 2014, pp. 343–354. doi:10.1007/978-3-662-45803-7_29.

[33] T. Bläsius, M. Krug, I. Rutter, D. Wagner, Orthogonal graph drawing with flexibility constraints, Algorithmica 68 (4) (2014) 859–885. doi:10.1007/s00453-012-9705-8.

[34] T. Bläsius, S. Lehmann, I. Rutter, Orthogonal graph drawing with inflexible edges, Comput. Geom. 55 (2016) 26–40. doi:10.1016/j.comgeo.2016.03.001.

[35] J. Cardinal, M. Hoffmann, V. Kusters, C. D. Tóth, M. Wettstein, Arc diagrams, flip distances, and hamiltonian triangulations, CoRR abs/1611.02541.

[36] R. Fulek, M. J. Pelsmajer, M. Schaefer, D. Stefankovic, Hanani-tutte and monotone drawings, in: P. Kolman, J. Kratochvíl (Eds.), WG, Vol. 6986 of LNCS, Springer, 2011, pp. 283–294. doi:10.1007/978-3-642-25870-1_26.

[37] S. Felsner, Geometric Graphs and Arrangements, Advanced Lectures in Mathematics, Vieweg, 2004. doi:10.1007/978-3-322-80303-0.

[38] W. Schnyder, Embedding planar graphs on the grid, in: D. S. Johnson (Ed.), SODA, SIAM, 1990, pp. 138–148.

[39] M. Chrobak, T. H. Payne, A linear-time algorithm for drawing a planar graph on a grid, Inf. Process. Lett. 54 (4) (1995) 241–246. doi:10.1016/0020-0190(95)00020-D.